ELSEVIER

Journal of Molecular Catalysis A: Chemical 95 (1995) 61–74

JOURNAL OF MOLECULAR CATALYSIS A: CHEMICAL

Effect of Fe-ZSM-5 zeolite on the photochemical and biochemical degradation of 4-nitrophenol

C. Pulgarin [a], P. Peringer [a], P. Albers [b], J. Kiwi [c,*]

[a] *Institut de Génie l'Environment, Laboratoire de Génie Biologique, Ecole Polytechnique Fédérale de Lausanne CH-1015 Lausanne, Switzerland*

[b] *Degussa AG, Wolfgang, Hanau 1, Germany*

[c] *Institute de Chimie Physique, Ecole Polytechnique Fédérale de Lausanne, CH-1015 Lausanne, Switzerland*

Received 17 June 1994; accepted 16 August 1994

Abstract

This study presents a novel approach for the degradation of 4-nitrophenol using Fe-ZSM-5 zeolite (Fe–zeolite). The influence of temperature, light, H_2O_2 concentration and amount of 1.5% Fe–zeolite catalyst used during the reaction has been systematically studied. A solution containing 4-nitrophenol (3.6×10^{-3} M), 1.5% Fe–zeolite (1.375g/l) and H_2O_2 (1.3×10^{-2} M) photodegraded the pollutant in $\approx$8 h at 35°C as seen by HPLC. The same solution needed $>$12 h to attain complete mineralization as shown by TOC experiments. Therefore CO_2 is the major oxidation product. The amount of H_2O_2 used in the reaction was monitored throughout. Based on NMR experimental results the $^{\cdot}OH$ radicals are considered to be reactive species responsible for the degradation reactions. Physical insight is given through a model for the surface reaction taking place. This model suggests that the degradation is partly due to the zeolite surface. Biodegradability of 4-nitrophenol was monitored by biochemical oxygen demand (BOD), chemical oxygen demand (COD) and dissolved organic carbon (DOC).

Keywords: Biochemical degradation; Degradation; Fe-zeolite; 4-Nitrophenol; Photocatalysis; Zeolite

1. Introduction

Nitrophenol compounds are common toxic, industrial and persistent pollutants [1,2] and it is desirable to degrade them to concentrations of less than 20 ppb [2] in water reservoirs. Direct photolysis has not been found to be effective in degrading 2,3,4-nitrophenols [3,4]. Until now only a few studies have been published using Fenton and photo-Fenton reactions in the degradation of pollutants [5–15]. In the particular case of nitrophenol, TiO_2 dispersions have been reported recently [6,16].

The aim of this study is threefold: (1) To use oxidizing systems containing Fe in a zeolite frame. (2) To seek the possibility of achieving total mineralization of this pollutant with this new material. (3) To assess the participation of photo-Fenton reactions in 4-nitrophenol degradation.

Different values for 4-nitrophenol biodegradation (up to 4.5 days) have been reported [17]. In this study we carried out biodegradation experiments to compare results obtained with photocatalytic degradation under similar experimental conditions. Photooxidation in water of 4-nitrophenol is reported to take from 6 weeks up to a year [18]. Another reason to undertake this study

* Corresponding author.

SSDI 1381-1169(94)00156-1

is that currently chlorine and hypochlorites are used to degrade organic pollutants. But these oxidative processes also induce dangerous halocarbon residues [9,19]. Therefore a study involving new methods to degrade phenols is warranted.

2. Experimental section

2.1. Materials

Hydrogen peroxide used was Fluka p.a. > 30%. 4-nitrophenol was also Fluka p.a. > 99% and was used without further purification. 1.5% Fe-ZSM-5 zeolite (from now on: Fe–zeolite) was provided by Degussa, Hanau 1, Germany, using as starting material zeolite with a module 28 in the SiO_2/Al_2O_3 ratio. This material was exchanged with $FeSO_4$ for 3 days keeping the pH at 3.9. Before ion-exchange, the zeolite was washed with a pH 5 buffer solution. After ion-exchange, the zeolites were thoroughly washed with distilled water and dried in air at 400K for 5 h.

2.2. Photoreactors and procedures

Photolysis experiments were carried out by means of a Hanau Suntest Lamp (AM1). The electrical power of this lamp was 2.1 kVA and the radiant flux entering the photolysis flasks were 80 mW/cm^2. Photolysis was carried out in 60 ml Pyrex flasks with $\lambda > 290$ nm. Fe^{3+} ions were analysed by complexation with thiocyanate at 476 nm [19,20] in a Hewlett-Packard instrument as stated below. The analysis of peroxide was carried out via $KMnO_4$ titration knowing that 2.5 mol of peroxide are oxidized by one mole of permanganate. The $KMnO_4$ consumed is estimated from the decrease in the optical absorption at 525 nm. The peroxide on the powder was analysed by dispersing the powder in water, adjusting pH 0 and measuring the permanganate consumed. The blank for the peroxide analysis has been carried out with 1.5% Fe–zeolite system stirred in the dark for the same period of time as the one under irradiation.

2.3. Analyses

High pressure liquid chromatography (HPLC) was carried out via a Varian 5500 unit. A Spherisorb silica column (HPLC Technology 5 ODS-2) with water–methanol gradient elution was used and the signal observed with UV detector at $\lambda = 315$ nm for 4-nitrophenol.

Total organic carbon (TOC) was monitored during degradation via a Shimadzu-500 instrument equipped with an automatic sample injector. Proton nuclear magnetic resonance (NMR) was carried out by means of a Bruker ACP-2000. Spectrometric analysis (OD) was performed via a Hewlett-Packard 386/20N diode array. Biological oxygen degradation (BOD) was carried out by means of a BSB Controller Model 1020 T (WTW). The unit was thermostated at 20°C and urban waste water after primary decantation was used as inoculum.

Using a Tecator titrator the nitrate is determined via the cadmium reduction method. The aqueous sample containing nitrate/nitrite is injected into the carrier stream which is merged with a second buffered carrier system. The nitrate is reduced to nitrite in a cadmium reducing column. On the addition of acidic sulphalinamide a diazo compound is formed, which then reacts with *N*-(1-naphtyl)-ethylene-diamine dihydrochloride provided from a second reagent stream. A purple azo dye is formed and the colour intensity is measured spectrophotometrically at 540 nm.

The peroxide remaining in the solution during irradiation was detected trough titration with permanganate of potassium. The samples taken for the analysis were centrifuged each time and the peak for permanganate was followed spectroscopically at 525 nm [21].

Photoelectron spectroscopy (XPS) was carried out using a Leybold Heraeus instrument and Mg $K_{\alpha,1,2}$ line at 1253.6 eV. The photoelectron spectrometer was evacuated to 2×10^{-8} mbar. Binding energies were referenced to the $4f_{7/2}$ level of Au at 83.8 eV. The quantitative evaluation of the data used polynomial fit with a Shirley-type background subtraction. The material was measured as

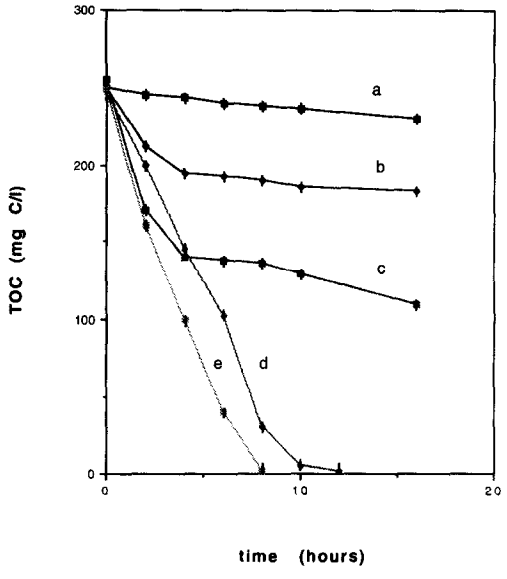

Fig. 1. Degradation of 4-nitrophenol (3.6×10^{-3} M) by TOC in the presence of zeolite (1.375 g/l) and H_2O_2 (1.3×10^{-2} M) as a function of time. (a) Zeolite undoped at 35°C under light, (b) 1.5% Fe–zeolite at 35°C in the dark, (c) 1.5% Fe–zeolite at 65°C in the dark, (d) 1.5% Fe–zeolite under light at 35°C, (e) 1.5% Fe–zeolite under light at 65°C.

powder in Au-coated stainless steel supports. Secondary ion mass spectrometry (SIMS) was recorded with Ar-ion gun (Leybold) IQ 12/38, 3 keV provided with a quadrupole mass spectrometer (Balzers) QM511. Atomic absorption (AAS) was carried out by means of a Philips 800-20 instrument.

3. Results and discussion

3.1. Kinetics of the photocatalytic disappearance of 4-nitrophenol. Effect of the various parameters on the observed rate of degradation

Fig. 1 presents the effect of temperature and light irradiation on the 4-nitrophenol degradation when zeolite and 1.5% Fe zeolite is used. Trace (a) shows the results for a 4 nitrophenol (3.6×10^{-3} M) solution containing zeolite (1.375 g/l) and H_2O_2 (1.3×10^{-2} M) under light illumination. Trace (a) shows that the degradation via zeolite alone under light at 35°C is less than 5% as reflected by the total organic carbon(TOC) up to 20 h. Trace (b) shows that 1.5% Fe–zeolite in a dark reaction induces up to 27% degradation at 35°C. A similar reaction is shown in trace (c) for the 1.5% Fe–zeolite at 65°C. Up to 52% degradation of 4-nitrophenol is observed in this case. Light induced reactions are shown in traces (d) and (e). Irradiation in trace (d) shows total mineralization in 12 h at 35°C, but in (e) this mineralization occurs faster in only 8 h at 65°C. Fig. 1 therefore shows the beneficial effect of light and thermal activation in 4-nitrophenol degradation. Zeolite alone as shown in Fig. 1 trace (a) points out that adsorption of the phenol on the surface-OH groups do not by themselves actively promote 4-nitrophenol degradation under light.

In Fig. 1 at 35°C it can be seen that mineralization took place over a 12 h period. Since the UV component of the solar spectrum ($\lambda > 290$ nm) is sufficient, a practical application of this method in waste water treatment cannot be discounted. Complete mineralization was not observed in the dark at 35°C or 65°C in Fig. 1 because some of the ring-cleavage products were unable to reduce Fe^{3+}.

The peroxide remaining in solution decreased less than 10% over a ten hour period. This is reflected by a constant peak for permanganate at 525 nm when 25 μl of peroxide (in 80 ml solution) was added during the photolysis in Fig. 1. When a one time initial injection of peroxide was applied we get a peak growth for permanganate of the order of 70% over a 15 h period. This is due to the increased amount of permanganate not used up during the titration. The observed stoichiometry reveals several complex redox reactions taking place during 4-nitrophenol degradation and such a scheme will proposed later in this study.

To follow specifically the degradation of 4-nitrophenol HPLC analysis was carried out at 315 nm. The results are shown in Fig. 2. The solution used had the same composition as in Fig. 1. Complete degradation of 4-nitrophenol was observed in 4 h at 65°C and over 8 h at 35°C.

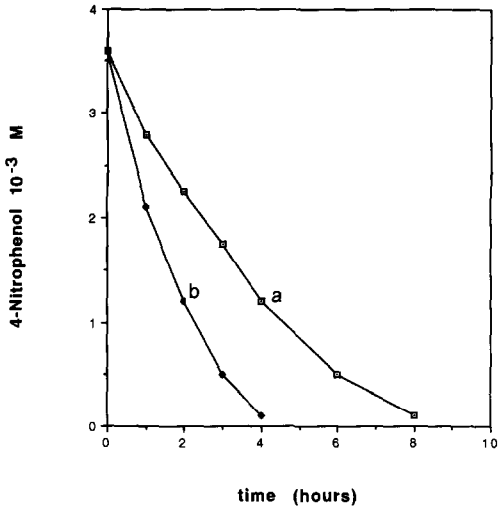

Fig. 2. Photodegradation of 4-nitrophenol (3.6×10^{-3} M) in the presence of 1.5% Fe–zeolite (1.375 g/l) and H_2O_2 (1.3×10^{-2} M) as detected by HPLC. (a) Under light at 35°C, (b) under light at 65°C.

Fig. 3 shows the first order plot for the kinetics already reported in Fig. 2. It is seen from Fig. 3 that a good straight line fit is obtained for the experimental points in both cases. In the case of trace (b) at 65°C the photodegradation is faster. A correlation factor of $R>99\%$ was found. The decomposition rate constants were 0.31 h^{-1} at 35°C and 0.60 h^{-1} at 65°C. These values obtained were seen to depend on the pH of the solution, the mass of Fe–zeolite used during the irradiation, and the intensity of the light applied to the suspension under study.

The pseudo-first order fit of the experimental values observed in Fig. 3 could be indicative of steady state ·OH radical concentration occuring during photodegradation. The experiments in Fig. 3 used a 4-nitrophenol concentration of 3.6×10^{-3} M. The reaction rate for the degradation reported in Fig. 3 can be stated:

$$rate = dC_{4\text{-nitrophenol}}/dt = kC_{4\text{-nitrophenol}} \quad (1)$$

where k = pseudo-first order rate constant and $C_{4\text{-nitrophenol}}$ is equal to the volume concentration of 4-nitrophenol in solution. In Eq. 1 if a steady state ·OH radical concentration is attained then:

$$k = k'C_{OH} \quad (2)$$

$$rate = k'C_{OH}C_{4\text{-nitrophenol}} \quad (3)$$

The photoassisted overall mineralisation of 4-nitrophenol therefore could be written:

$$C_6H_5NO_3 + 6\cdot OH(3H_2O_2) + 11/2O_2 \rightarrow$$

$$6CO_2 + 5H_2O + HNO_3 \quad (4)$$

Due to the values presented in Fig. 1, the mineralization of 4-nitrophenol proceeds with a yield of around 0.1 kWh/ppm C/l.

Fig. 4 presents the TOC values in (mg C/l) after 7 h for a solution 4-nitrophenol (3.6×10^{-3} M) containing 1.5% Fe–zeolite (1.375 g/l) and diverse amounts (added each hour) of H_2O_2 at 35°C under light. It is readily seen that when higher doses of H_2O_2 are injected a plateau is reached at 220 μl H_2O_2/h. This result is consistent with trace (d) in Fig. 1. Moreover, these results confirm that H_2O_2 as a reagent determines the kinetics of degradation in addition to the initial amount of 4-nitrophenol and Fe–zeolite used as shown next in Fig. 5.

Fig. 5 presents the experimental results of runs using slurries containing 4-nitrophenol (3.6×10^{-3} M), H_2O_2 (3×10^{-2} M) and 1.5% Fe–zeolite concentrations from 0.2 to 2.5 g/l.

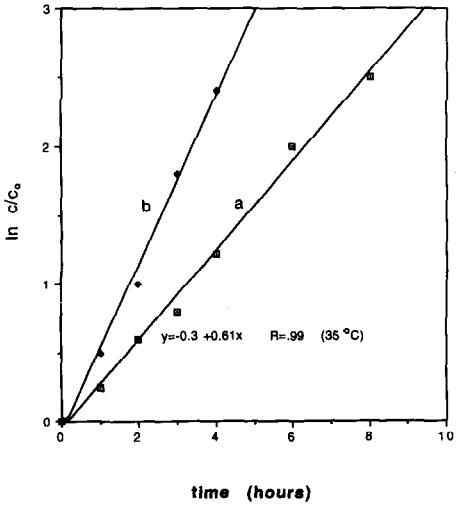

Fig. 3. First order plot for kinetics of 4-nitrophenol (3.6×10^{-3} M) in the presence of 1.5% Fe–zeolite (1.375 g/l) and H_2O_2 (1.3×10^{-2} M) under light: (a) 35°C, (b) 65°C.

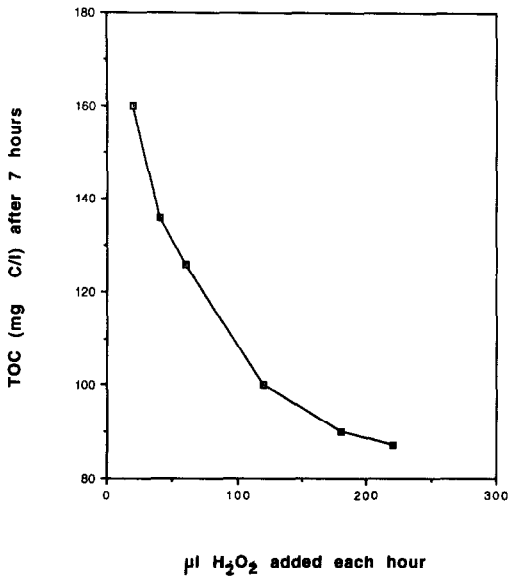

Fig. 4. TOC values (mg C/l) after 7 h when a solution of 4-nitrophenol (3.6×10^{-3} M) is photodegraded in presence of 1.5% Fe–zeolite (1.375 g/l) and H_2O_2. The H_2O_2 was added hourly as indicated.

These results show the effect of the catalyst concentration on the rate constant. Therefore the reaction takes place as a function of the amount of Fe–zeolite used. BET area could not be obtained unequivocally for the Fe–zeolite used since this material revealed itself to be microporous with a

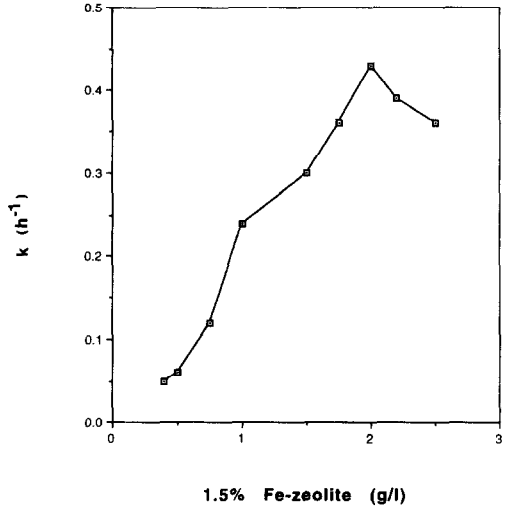

Fig. 5. Dependence of the first order rate constant (k) for 4-nitrophenol (3.6×10^{-3} M) photodegradation on 1.5% Fe–zeolite concentration in the presence of H_2O_2 (1.3×10^{-2} M).

c value above 200. The type of isotherm obtained is susceptible to analysis if the value of c is below 100. According to BET theory the magnitude of c gives an indication of the adsorbent–adsorbate interaction energy. In our case this energy seems to be rather high. In Fig. 5 the first seven points are roughly aligned and therefore the observed rate constants are proportional to the mass (m) of the catalyst used. The ratio k/m corresponds to the specific rate constant per mass unit of Fe–zeolite used. Throughout this work, 1.375 g/l was subsequently used since it afforded good catalytic activity on the one hand, and good reproducibility on the other. At higher concentrations > 2.0 g/l a further increase of the catalyst produces an inner filter effect.

3.2. *Rate of Fe(III) dissolution during the photocatalytic experiments*

From Fig. 5 we observe that the rate constants for 4-nitrophenol degradation increases as the amount of Fe–zeolite is increased. To understand further this effect we irradiated a solution containing 1.5% Fe–zeolite (1.375 g/l) and H_2O_2 (1.3×10^{-2} M). This irradiation showed a concentration of Fe^{3+} in the solution of 2×10^{-5} M. We used this concentration of Fe ions added in a homogeneous solution run in the presence of 4-nitrophenol and H_2O_2 as in the run reported in Fig. 1d) at 35°C. The results are shown in Fig. 6a). It is readily seen that a 50% decrease in TOC values takes place in 24 h. This is much less than the decrease observed in Fig. 1d) showing that the surface contribution of the Fe–zeolite is the controlling factor in the observed photodegradation. Further, we carried out homogeneously the same run adding 1.2×10^{-4} M Fe^{3+} since this is the maximum Fe ion concentration to be found in the solution when zeolite (1.375 g/l) is used (Fig. 1d). A 95% decrease in the TOC values is observed in this case in Fig. 6, trace b), but over 24 h, indicating a much longer time than when Fe–zeolite was used as seen in Fig. 1d).

Fig. 7 indicates the concentration of Fe ion when a solution of 4-nitrophenol (3.6×10^{-3} M),

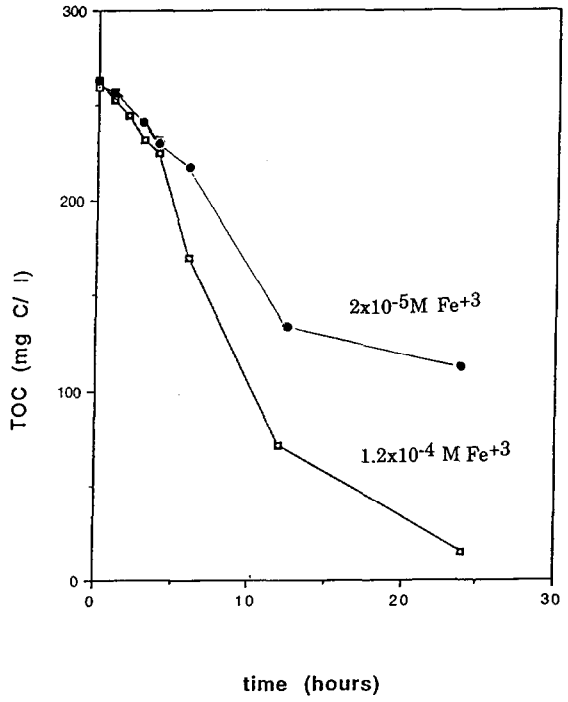

Fig. 6. Effect of Fe^{3+} ion concentration on the degradation of 4-nitrophenol (3.6×10^{-3} M) in a homogeneous reaction adding H_2O_2 (1.3×10^{-2} M) under light at 35° (a) 2×10^{-5} Fe^{3+} M, and (b) 1.5×10^{-4} Fe^{3+} M.

H_2O_2 (1.3×10^{-2} M) and Fe–zeolite (1.375 g/l) is reacted under light or in the dark as a function of time at different temperatures. It is readily seen that the degradation taking place is light and temperature dependent. In the dark an equilibria gets established at about 5 h. The observed values suggest that an equilibria is established after this time at the surface and that this surface is active at later times in the reaction. The values observed under light in Fig. 7 show that 4-nitrophenol and H_2O_2 intervene actively in the Fe dissolution. Photocorrosion in Fe-containing systems have been studied before in our laboratory [21,22]. Up to 64% of the initial Fe^{3+} (Fig. 7) available in the 1.5% Fe–zeolite enters the solution after 15 h (light, 35°C). In separate experiments a sample of 1.5% Fe–zeolite was heated in air and turn red–brown, the typical colour of Fe_2O_3. Therefore we cannot discount the existence of a small amount of Fe_2O_3 on the surface of the 1.5% Fe–zeolite. Due to the semiconductor character of the Fe_2O_3 present the conduction band reaction which occurs in the presence of H_2O_2 consists in the reaction of lattice or surface Fe (III) to Fe(II) [21,22].

$$Fe_2O_3/Fe(III)\,\text{lattice/surface} \xrightarrow{\text{light}} + C_6H_4(OH)NO_2 \rightarrow$$

$$Fe_2O_3/Fe(II)\,\text{lattice/surface} + C_6H_3(OH)NO_2 + H^+ \quad (5)$$

Incident photons initiate a series of reactions that ultimately transfers an electron from the iron oxide lattice to a Fe(III)-centered orbital. In the presence of 4-nitrophenol a free radical Eq. 5 and Fe(II) is formed. Indirect evidence for the 4-nitrophenol derived radical in Eq. 5 comes from the observation of many peaks by HPLC techniques close to the main 4-nitrophenol peak. The long lived substances relating to this peak correspond to the decomposition products of this intermediate radical. The recycling of the Fe(II) takes place subsequently in the presence of H_2O_2 through a surface redox reaction [23–25] with a rate $k=76$ ($M^{-1}\,s^{-1}$).

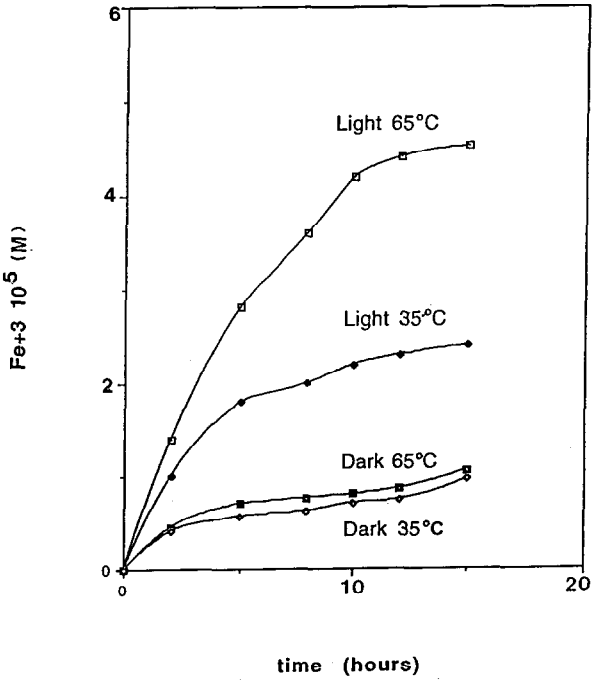

Fig. 7. Concentration of Fe^{3+} ions in solution when the solution used in Fig. 2 is reacted in the dark and under light at 35° or 65°C.

$$\text{Fe(II) lattice/surface} + H_2O_2 \xrightarrow{\text{light}} \text{Fe(III) lattice/surface} + OH^{\cdot} + OH^- \quad (6)$$

The dissolution of Fe(III) from the surface into the bulk aqueous phase is shown by:

$$\text{Fe(III) lattice/surface} \rightarrow \text{Fe(III) aqueous} \quad (7)$$

If the OH radicals are generated close to the surface of the zeolite then they may interact with the iron centers and produce an analogue of the FeO^{3+} center at the natural enzyme as shown below in Eq. 8.

$$2\text{Fe(III) aqueous} + 2\,{}^{\cdot}OH \rightarrow FeO^{3+}/FeO^{2+} + H_2O \quad (8)$$

In our case the reducing cofactor would be 4-nitrophenol as shown previously in Eq. 5. The generation in situ of iron species with valences Fe(IV/V) as suggested above, has been reported before [26,27]. We could not check out these species since they have only been stabilized in relatively complicated perovskite structures at higher temperature and detected by EPR.

Fig. 8 shows the nitrate evolution when a solution containing 4-nitrophenol (3.6×10^{-3}), H_2O_2 (1.3×10^{-2}) and catalyst (1.375 g/l) was photolyzed at 35°C. Nitrate ion was analyzed during the course of these experiments (see Experimental part). After about 14 h a level of 144 mg nitrate/l was attained equal to the maximum possible. The results shown in Fig. 1d) involving 4-nitrophenol degradation, correlate well with the time span of Fe ion growth reported in Fig. 7 and the appearance, growth and equilibration of nitrate ion shown in Fig. 8. These data support the proposed mechanism for the degradation taking place.

Another important observation to make here is that a very low concentration of Fe^{3+} ions is active in homogeneous reactions during the destruction of nitrophenols and related organic molecules [12–14]. These ions would participate in reactions (9) and (10). Fe^{3+} ions would initiate decomposition of H_2O_2 [8,13,22]:

$$Fe^{3+} + H_2O_2 \rightarrow HO_2^{\cdot} + H^+ + Fe^{2+} \quad (9)$$

with Fe^{2+} ion producing $^{\cdot}OH$ radicals in addition to eq (6):

$$Fe^{2+} + H_2O_2 \rightarrow Fe^{3+} + {}^{\cdot}OH + OH^- \quad (10)$$

Fe^{3+} ions were evaluated immediately to avoid the effect reported by Eq. 10 on the concentrations of Fe^{3+} ion dissolution in Fig. 7.

$$Fe^{3+} + H_2O + h\nu \rightarrow Fe^{2+} + OH + H^+ \quad (11)$$

Continuous photoproduction of Fenton reagent takes place during 4-nitrophenol degradation. Several processes take place simultaneously involving 4-nitrophenol, H_2O_2 and the $Fe(OH)^{2+}$ charge transfer band with $\epsilon = 2050\ M^{-1}\ cm^{-1}$ at 295 nm [10]. The absorption of the charge transfer band is important since the degradation reported for 4-nitrophenol by the near UV light could also be found in sunlight in the 290–400 nm region, close to the transfer complex peak of $Fe(OH)^{2+}$.

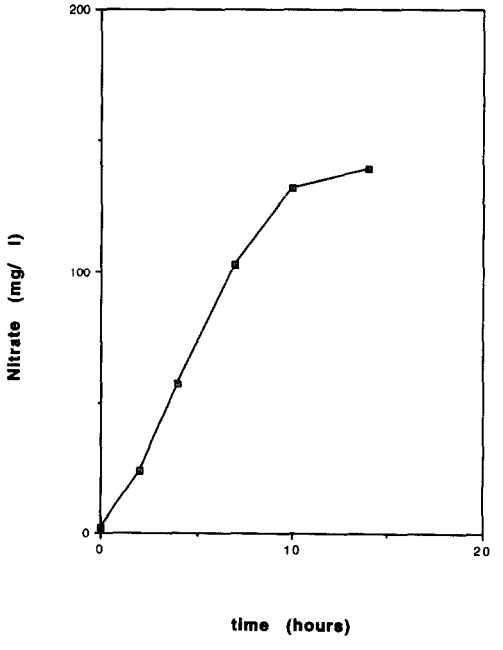

Fig. 8. Concentration of nitrate as a function of time when a solution like the one used in Fig. 2 is irradiated at 35°C.

3.3. Observation of the photocatalytic decomposition of 4-nitrophenol at 35°C under light by ^{1}H-NMR spectroscopy

The products of the photocatalyzed degradation reported in Fig. 1 trace (d) were examined by ^{1}H-NMR spectroscopy and are shown in Fig. 9. In spectrum (a), the proton signals are seen at zero irradiation time for residual water protons (4.7 ppm), protons close to the OH group (7 ppm) and close to NO_2 group (8 ppm). After 1.5 h irradiation spectra (b) shows the existence of the

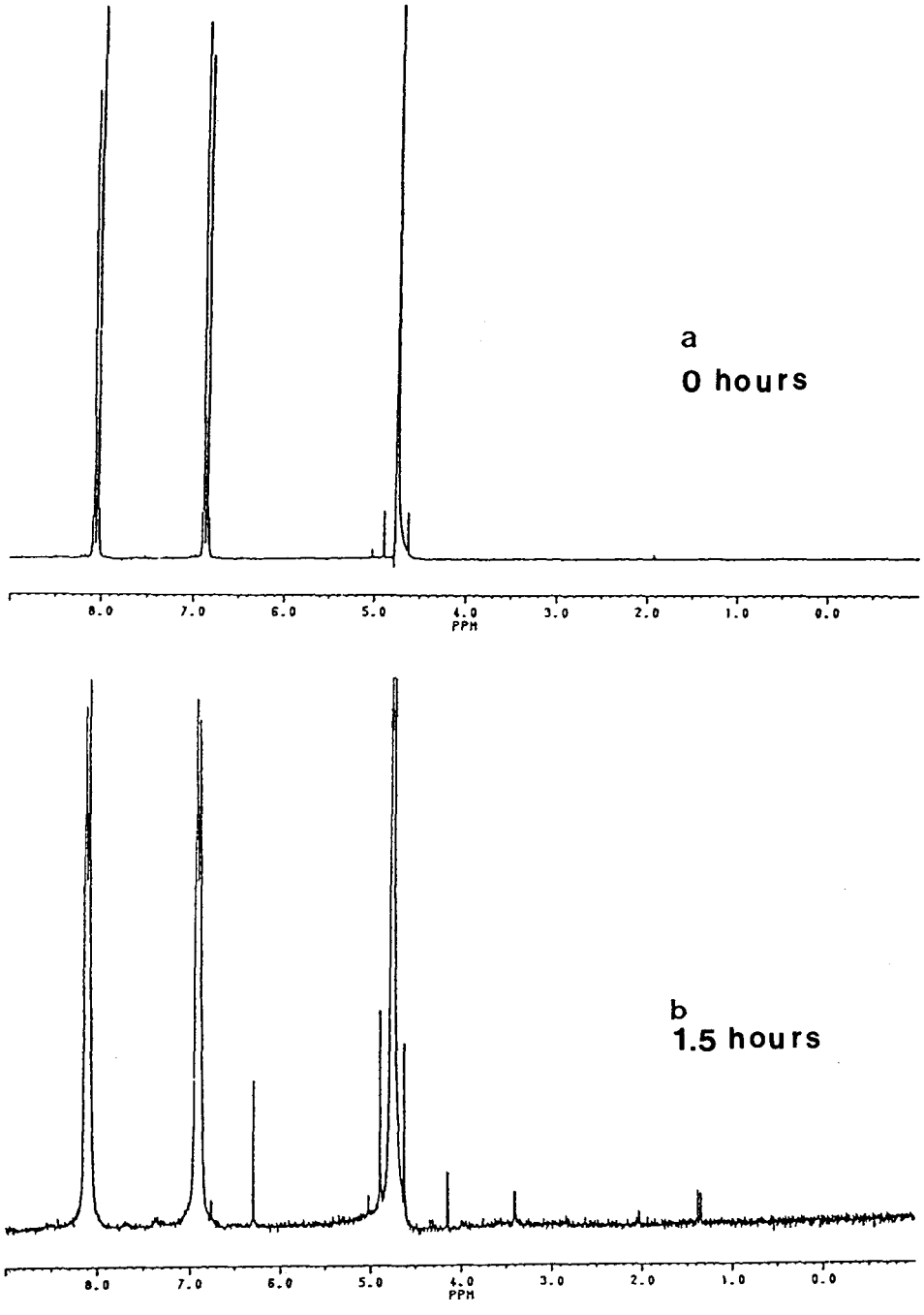

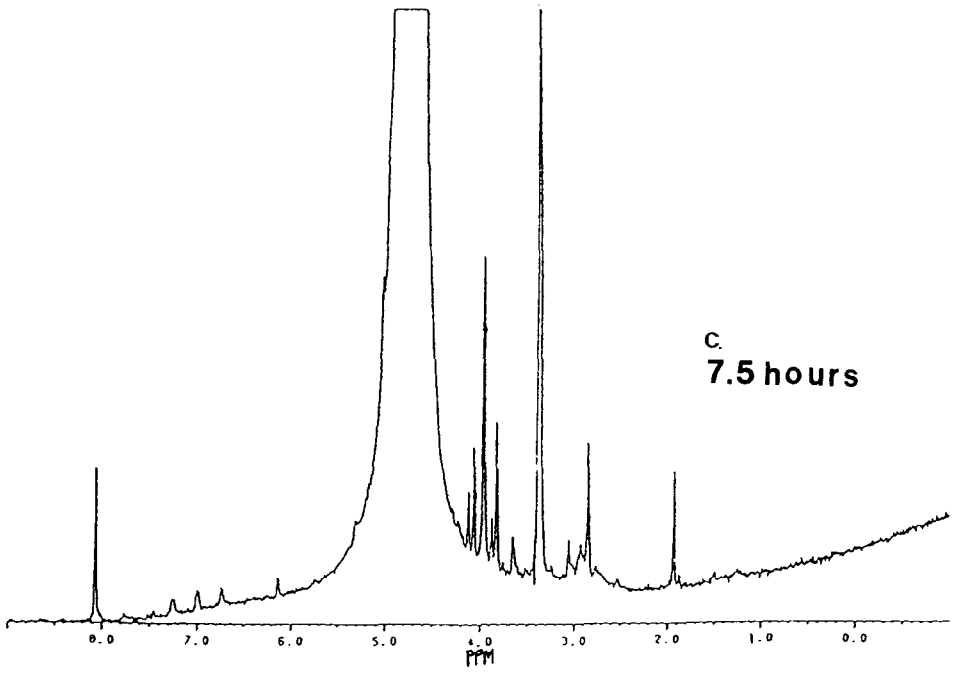

Fig. 9. ^{1}H-NMR spectra of 4-nitrophenol photodegraded at 35° with 1.5% Fe–zeolite a period of (a) 0 (b) 1.5 h (c) 7 h.

aromatic group and the appearance of signals due to vinyl protons (6.3 ppm). Weak signals due to aliphatic photons also appear between 3 and 4.2 ppm. After 7–8 h (see Fig. 2) the aromatic groups are almost destroyed and the proton signals for methylene groups (3.8 ppm) and aliphatic protons become dominant. Since the TOC values trace (d) in Fig. 1 decreases by 45% in 1.5 h, but the aromatic groups are observed by ^{1}H-NMR spectrum, it is suggested that the decomposition step leading to $CO_2 + H_2O$ is much faster than the hydroxylation step due to $^{\cdot}OH$ attack on the 4-nitrophenol ring. There has been general agreement on the hydroxylation step of the aromatic ring as a primary step in phenol decomposition reactions [3,9,22]. These results have been confirmed following the decrease in the optical absorption of 4-nitrophenol at 315 nm.

Comparing the TOC (mg C/l) values obtained for the light induced degradation of 4-nitrophenol trace (d) in Fig. 1 and trace (a) in Fig. 2 obtained by HPLC at 35°C, it is readily seen that a higher rate is taking place in Fig. 2 as compared to Fig. 1. Two processes are taking place side by side leading to the degradation of 4-nitrophenol. In effect we have observed CO_2 evolution from the start until total mineralization as shown by Eq. 4. The first process is faster than the rate subsequently observed for the total degradation. These processes could be represented in the reations [12–16]. The rate found for k_{12} by HPLC (Fig. 2) is indicative of an easier process than the subsequent decomposition of aliphatic intermediates in 4-nitrophenol degradation. Hydroxylation of the initial substance has previously been studied and reported for phenol compounds [9–13]. Intermediates like benzoquinone, nitrohydroquinone, 4-nitrocatechol and 4-nitrosophenol have already been reported during 4-nitrophenol degradation [3,6,10].

Therefore we could suggest in Scheme 1 that $k_{12} \approx k_{13} \approx k_{14} > k_{15}$. Scheme 1 proposed is consistent with previous results found in the degradation of phenolic compounds [5–16]. Fig. 2 indicates that at 35°C and 65°C the decomposition of 4-nitrophenol and cyclic intermediates produced during the reaction is faster than the mineralization of the aliphatic intermediates as shown in the

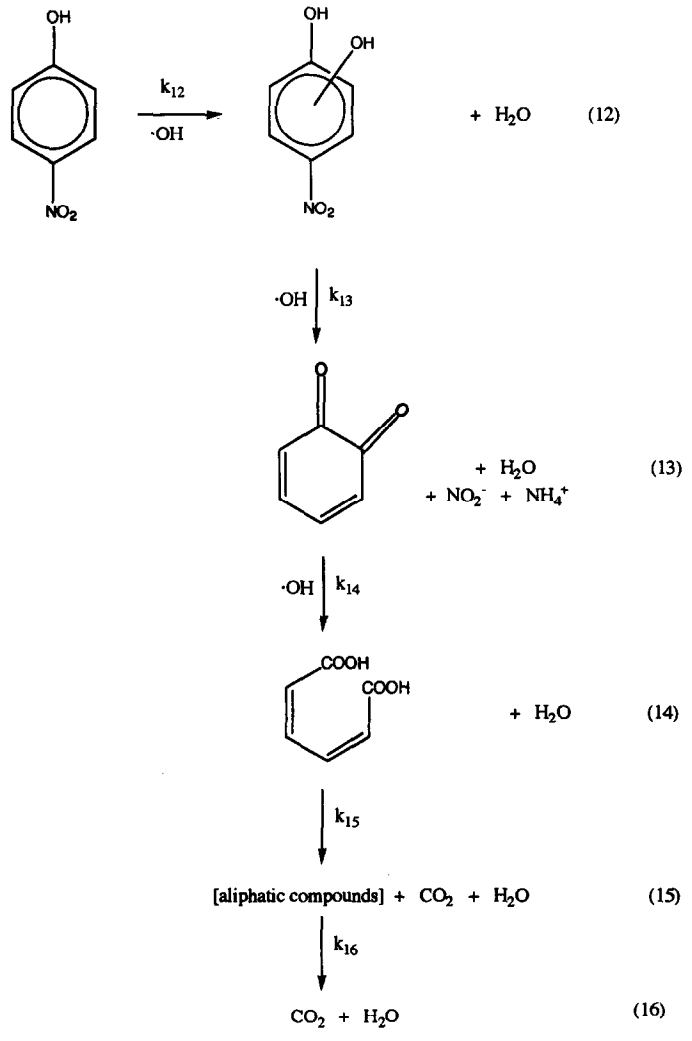

Scheme 1.

last two steps of the scheme. Moreover, under light many ·OH radicals are formed in comparison with the dark Fenton reaction where only a single radical is formed for each Fe ion [13]. The benzophenones shown in the scheme are known to be unstable [9].

Results have been published on the degradation and photodegradation of 4-nitrophenol. Reference [6] reports the degradation of this substance only via Fenton processes using a different lamp and different concentrations of initial reagents. Recently Augugliaro et al. also reported 4-nitrophenol photodegradation using TiO_2 suspensions over periods > 5 h [16].

3.4. Biodegradability tests

Biochemical oxygen demand (BOD) for 4-nitrophenol (2.3×10^{-3} M) in waste water bacteria media is shown in Fig. 10. The aim was to quantify the oxygen utilized during the degradation of 4-nitrophenol by waste water bacteria. Three bottles were taken for each sample containing standard N, P nutrients required during the biological process. Sewage water was taken after the initial decantation process of the Vidy (VD, Switzerland) biological waste water treatment plant. This solution was further decanted 24 h and filtered through cotton. The oxygen consumed

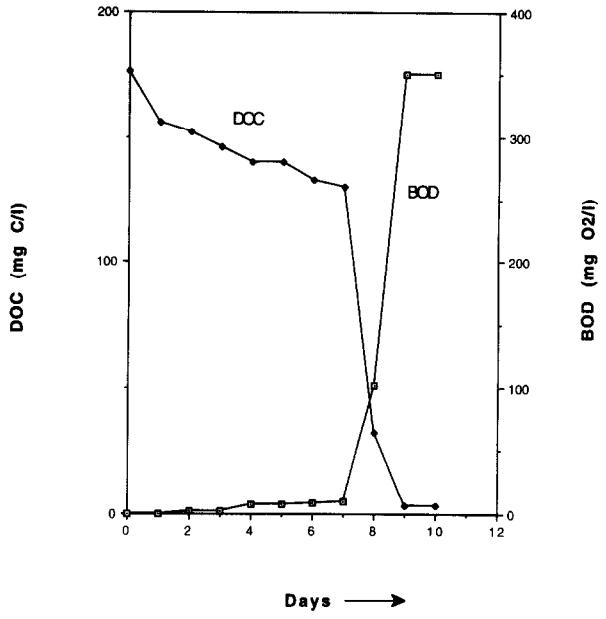

Fig. 10. Biochemical oxygen demand (BOD) and dissolved organic carbon (COD) as a function of time during 4-nitrophenol biodegradation.

was measured via the instrument indicated in the experimental part. Blank BOD reference runs are carried out with bacteria only. The formula used to calculate the BOD reported in Fig. 9 is:

$$\mathrm{BOD} = \frac{[\mathrm{BOD\ measured} - 0.01(\%\mathrm{inocolum} \times \mathrm{BOD\ inoculum})]}{(100 - \%\ \mathrm{inoculum}) \times 0.01}$$

The percentage of inoculum used was 20%. The 4-nitrophenol solutions used here contained 340 mg/l or the equivalent of 175 mg C/l. This solution has a chemical oxygen demand (COD) of 600 mg O_2/l. During the 10 day degradation period, the dissolved organic carbon (DOC) was monitored. Fig. 10 shows a slow adaptation period for bacterial action up to 7 days. After 7 days the BOD values increase from 2 mg O_2/l/day to 180 mg O_2/l/day and DOC consumption from 6 mg C/l/day to 65 mg C/l/day. This means that the BOD values increase by a factor of 90 from the adaptation period to the exponential growth period. The ratio BOD_9/COD obtained is 0.62 which corresponds to generally accepted rate of biodegradable substances after microorganisms adaptation [18,19]. BOD_9 is the biochemical oxygen demand observed after 9 days.

Fig. 11 presents the results for 4-nitrophenol in a bacterial system as reported in Fig. 10. But light pretreatment has been applied during 8 h in the presence of Fe^{3+} ions and H_2O_2 as reported in Fig. 1, trace (d). It was intended to test the bac-

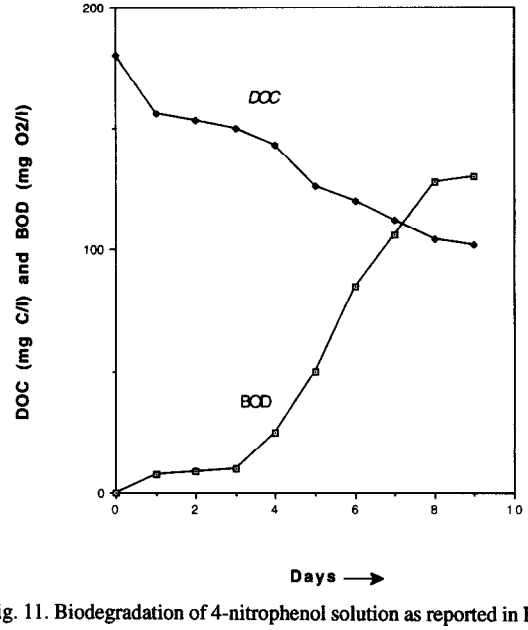

Fig. 11. Biodegradation of 4-nitrophenol solution as reported in Fig. 9 but applying photo-Fenton pretreatment for 8 h. For other experimental conditions see text.

Table 1
XPS values for the surface area of the elements found on 1.5% Fe–zeolite as a function of time (in %)

Element	Time (h)			
	0	4	8	12
Na	–	–	–	–
Fe	0.11	0.10	0.10	0.07
O	61.5	59.4	56.3	46.2
C	1.52	3.28	7.28	23.9
Cl	–	–	–	–
Si	35.3	35.0	34.3	28.2
Al	1.67	1.60	1.62	0.92
N	–	0.52	0.61	0.75

terial action on systems where the aromatic ring of the 4-nitrophenol has been already degraded (see Fig. 9). Fig. 11 shows that the products formed in this case are less biodegradable than when no photo-Fenton pretreatment was used (Fig. 10). In this case the initial solution used had a dissolved organic carbon (DOC) of 180 mg C/l and a chemical oxygen demand (COD) of 450 mg O_2/l. Fig. 11 shows that a BOD_9 of 128 mg O_2 was attained. This indicates a BOD_9/COD value of only 0.28. Fig. 11 shows that only 70 mg C/l is biodegraded during 9 days. Therefore the photo-Fenton treatment leads to the formation of intermediates not readily attacked by bacteria. Accelerated bacterial action on 4-nitrophenol after photo-Fenton pretreatment was not observed here. We have recently reported [7,8] that photocatalytic pretreatment is beneficial for bacterial degradation in water treatment.

3.5. Characterization of a Fe–zeolite catalyst used in photodegradation by X-ray photoelectron spectroscopy (XPS) and secondary ion mass spectroscopy (SIMS)

Tables 1 and 2 present the XPS results on the 1.5% Fe–zeolite after an experimental run for 8 h under the conditions outlined in Fig. 1 trace (d). Although the total content of Fe in the bulk of the fresh Fe–zeolite is 1.5% XPS showed values around 0.1%. XPS measures the percentage area of Fe ions on the surface. As stated previously in the experimental section, during the preparation of the catalyst, the Fe ions exchange into the zeolite lattice and only minor fractions remain on the surface, accessible to the XPS analysis. Table 1 shows that the iron values decrease from 0.11% to about 0.07% during the 12 h of reaction time. This is consistent with the photodissolution results (for the reaction) already reported in Fig. 7.

The nitrogen values on the catalyst surface are seen in Table 1 to increase as the reaction proceeds due to efficient 4-nitrophenol decomposition on the Fe–zeolite. The binding energies for the peaks observed after the charging correction [28] for N in nitrates was 407 eV and for nitrites 403 eV. The available peaks indicated the total decomposition of the parent compound (nitrophenol) since no other N-compounds were detected. Table 1 also shows that carbon concentration on the surface increased 15 times during the reaction time due to efficient nitrophenol decomposition.

Table 2 presents the results for the sample shown in Table 1 but having added 36 mg of $NaClO_4$ per 110 mg 1.5% Fe–zeolite. Perchlorate is a non-complexing anion. Due to the added salt a marked increase in Na and Cl on the catalyst surface is observed. The absence of surface-N demonstrates that N decomposition products of 4-nitrophenol are missing. A modest increase in surface C values is also observed. Under these conditions the the reaction was four times less effective than when $NaClO_4$ was absent. This negative effect observed is due to the increased ionic strength affecting the catalyst. Less C and no N

Table 2
XPS values for the surface area of the elements found on 1.5% Fe–zeolite as a function of time in the presence of $NaClO_4$ (in %)

Element	Time (h)			
	0	4	8	12
Na	3.13	7.23	4.93	6.07
Fe	0.15	0.16	0.13	0.08
O	51.5	44.0	44.6	44.7
C	11.6	17.6	18.2	19.2
Cl	3.24	7.63	5.18	6.76
Si	29.3	22.5	25.7	22.5
Al	1.10	0.90	1.28	0.70

Table 3
Secondary ion mass spectroscopy (SIMS)

Sample	Si^+/Fe^+ signal
zeolite, unloaded	150
zeolite + 1.5% Fe	54
after 4 h synthesis	58
after 8 h synthesis	60
after 12 h synthesis	78

deposits due to 4-nitrophenol decomposition are reported in Table 2. The evaluation of Fe signals of the catalyst yield binding values around 710.6 eV. This indicates that Fe(III) is the active species in the reaction and that it is present in the top atomic layers of the catalyst.

The secondary Ion Mass Spectroscopy technique results (SIMS) are seen in Table 3. They confirmed the trends observed by XPS presented in Table 1. The trend in Si^+/Fe^+ shows that Fe ions are lost during the reaction in the 50 nm upper layer region of the zeolite as studied by this technique. Comparison, e.g., of the SIMS spectra of the samples taken after 8 and with those taken after 12 h shows, that the relative intensities observed e.g. for SiO_2^- or SiO_3^- change, whereas the signals for FeO^- remain constant. This result demonstrates, that Fe loss of the surface takes place but that inside the zeolite the Fe is intact.

4. Conclusions

The present study reports for the first time on the action of Fe–zeolites in the photooxidation of 4-nitrophenol. At pH 3.0 approximately 3 mol of H_2O_2/mol of 4-nitrophenol were required under light to remove all the aromatic intermediate compounds from the solution. The surface of the zeolite apparently acts directing the substrate to the zeolite interface. During the time of 4-nitrophenol degradation concomitant Fe ion and nitrate ion growth was observed. This allowed the formulation for a possible mechanism for the observed degradation. The degradation proceeds through hydroxylation of the ring leading to cleavage and mineralization as observed by NMR techniques. The information presented here shows that the rate of destruction of 4-nitrophenol is a multistep process whose rate depends on the amount of zeolite, 4-nitrophenol, peroxide concentration and the temperature used The observed rates are a composite of the rates of the surface reaction, the dark reaction and the photoreactions taking place.

Acknowledgements

We thank J.-Paul Schwtzguébel for his help with the nitrate analysis and the Swiss National Science Foundation for partial support of this work.

References

[1] M. Nagakawa and D. Crosby, J. Agric. Food. Chem., 22 (1974) 849.
[2] List of Worldwide Hazardous Chemicals and Pollutants, Lippincot Co., New York, 1990.
[3] A. Alif, P. Boule and J. Lemaire, J. Photochem. Photobiol. A, Chem., 50 (1991) 331.
[4] O. Legrini, E. Oliveiros and M.A. Braun, Chem. Rev., 93 (1993) 67.
[5] V. Augugliaro, L. Palmisano, M. Schiavello, A. Sclafani, G. Marchese and F. Miano, Appl. Catal., 69 (1991) 323.
[6] E. Lipczynska-Kochany, Chemosphere, 24 (1992) 1369.
[7] J. Kiwi, C. Pulgarin, P. Peringer and M. Grätzel, New. J. Chem., 17 (1993) 487.
[8] J. Kiwi, C. Pulgarin, P. Peringer and M. Grätzel, Appl. Catal. B, Environ., 3 (1993) 85.
[9] W., Mathews, in E. Pelizzetti and M. Schiavello (Eds.}, Photochemical Conversion and Storage of Solar Energy, Kluwer, Dordrecht, 1991.
[10] M. Halmann, J. Photochem. Photobiol, A. Chem., 66 (1992) 215.
[11] B. Faust and J. Hoigne, J. Atmos. Environ., 24A (1990) 79.
[12] E. Lipczynska-Kochany, Environ. Technol. Lett., 12 (1991) 87.
[13] G. Ruppert, R. Bauer and G. Heister, J. Photochem. Photobiol. A. Chem., 73 (1993) 75.
[14] C. Maillard, Ch. Guillard and P. Pichat, Chemosphere, 24 (1992) 1085.
[15] R. Zepp, F. Bruce and J. Hoigne, Environ. Sci. Technol., 15 (1992) 313.
[16] V. Augugliaro, M. Lopez, L. Palmisano and J. Soria, Appl. Catal. A., 101 (1993) 7.
[17] P. Pitter and V. Chudoba, Biodegradability of Organic Substances in the Aquatic Environment, CRC Press, Boca Raton, FL, 1990.

[18] P. Howard, Handbook of Environmental Degradation Rates, Lewis, Washington, DC, 1989.
[19] K. Tanaka, T. Hisanaga and K. Harada, New. J. Chem., 13 (1989) 5.
[20] I. Kolthoff, E. Sandell, E. Meehan and S. Bruckenstein, Quantitative Chemical Analysis, McMillan, London, 1969, p. 1049.
[21] M. Grätzel, J. Kiwi, C. Morrison, R. Davidson and A. Tseung, J. Chem. Soc. Faraday Trans. 1, 81 (1985) 1883.
[22] J. Kiwi, C. Pulgarin and P. Peringer, Appl. Catal B., 3 (1994) 335.
[23] R. Williams, D. Reible, D. Wetzel and D. Harrison, Ind. Eng. Chem. Res., 26 (1987) 606.
[24] J. Kennedy and M. Anderman, J. Electrochem. Soc., 130 (1983) 848.
[25] G., Charlot, Les Reations Chimiques en Solution, Masson, Paris, 1969, p. 238.
[26] S.K. Lee, B.G. Fox, A.W. Froland, D.J. Lipscomb and E. Munck, J. Am. Chem. Soc., 115 (1983) 6450.
[27] L.J. Soubeyroux, B. Buffat, N. Chevrau and G. Demazeu, Physica B, 120 (1983) 227.
[28] L. Barr, in D. Briggs and M, Seah (Eds.), Practical Surface Analysis, Wiley, 1990, p. 412.